Available online at www.sciencedirect.com
SCIENCE DIRECT
Biochemical Pharmacology 69 (2005) 971–979
Biochemical Pharmacology
www.elsevier.com/locate/biochempharm

# L-Arginine regulates neuronal nitric oxide synthase production of superoxide and hydrogen peroxide

Pei Tsai[a,b,c], John Weaver[a,b,c], Guan Liang Cao[a,b,c], Sovitj Pou[c], Linda J. Roman[d], Anatoly A. Starkov[e], Gerald M. Rosen[a,b,c,*]

[a]Department of Pharmaceutical Sciences, University of Maryland School of Pharmacy, Baltimore, MD 21201, USA
[b]Medical Biotechnology Center, University of Maryland Biotechnology Institute, Baltimore, MD 21201, USA
[c]Center for Low Frequency EPR for In Vivo Physiology, University of Maryland School of Pharmacy, Baltimore, MD 21201, USA
[d]Department of Biochemistry, The University of Texas Health Science Center at San Antonio, San Antonio, TX 78229, USA
[e]Department of Anesthesiology, University of Maryland School of Medicine, Baltimore, MD 21201, USA

Received 27 October 2004; accepted 23 December 2004

**Abstract**

Tetrahydrobiopterin ($H_4B$) in the absence of L-arginine has been shown to be an important factor in promoting the direct formation of hydrogen peroxide ($H_2O_2$) at the expense of superoxide ($O_2^{\bullet-}$) by neuronal nitric oxide synthase (NOS1) [Rosen GM, Tsai P, Weaver J, Porasuphatana S, Roman LJ, Starkov AA, et al. Role of tetrahydrobiopterin in the regulation of neuronal nitric-oxide synthase-generated superoxide. J Biol Chem 2002;277:40275–80]. Based on these findings, it is hypothesized that L-arginine also shifts the equilibrium between $O_2^{\bullet-}$ and $H_2O_2$. Experiments were designed to test this theory. As the concentration of L-arginine and $N^{\omega}$-hydroxyl-L-arginine increases, the rate of NADPH consumption for $H_4B$-bound NOS1 decreased resulting in lower rates of both $O_2^{\bullet-}$ and $H_2O_2$ generation, while increasing the rate of nitric oxide ($^{\bullet}NO$) production. At saturating concentrations of L-arginine or $N^{\omega}$-hydroxyl-L-arginine (50 μM), NOS1 still produced $O_2^{\bullet-}$ and $H_2O_2$. Both L-arginine and $N^{\omega}$-hydroxyl-L-arginine have greater impact on the rate of generation of $O_2^{\bullet-}$ than on $H_2O_2$.


*Keywords:* L-Arginine; $N^{\omega}$-Hydroxyl-L-arginine; superoxide; Nitric oxide; Hydrogen peroxide; Neuronal nitric oxide synthase

## 1. Introduction

Neuronal nitric oxide synthase (NOS1) (EC 1.14.13.39) is a heme-containing protein that selectively produces nitric oxide ($^{\bullet}NO$) from L-arginine [1,2]. This enzyme is comprised of an N-terminal oxidase domain with binding sites for L-arginine and tetrahydrobioprotein ($H_4B$) and a C-terminal reductase domain with binding sites for FMN, FAD, and NADPH. The domains are connected by a $Ca^{2+}$/calmodulin binding region that allows electron transport through the enzyme [3,4]. In its functional state, NOS is a dimer in which electrons from one subunit of the oxygenase domain accepts electrons from FMN of the reductase domain of the other subunit [5–7]. This unique enzyme catalyzes a two-step monooxygenase reaction, converting L-arginine to $N^{\omega}$-hydroxyl-L-arginine, as an intermediate and then to L-citrulline and $^{\bullet}NO$ [8,9]. Neuronal nitric oxide synthase also generates superoxide ($O_2^{\bullet-}$) and hydrogen peroxide ($H_2O_2$) during enzymic cycling [10–15].

There are a number of control mechanisms that regulate NOS1 production of $^{\bullet}NO$, $O_2^{\bullet-}$, and $H_2O_2$. For instance, $H_4B$ appears to play a critical role in the NOS oxidation of L-arginine to $^{\bullet}NO$ and L-citrulline [15–23]. Similarly, this pterin, in the absence of this amino acid, promotes direct generation of $H_2O_2$ at the expense of $O_2^{\bullet-}$ [15]. Finally, L-arginine, by binding to NOS1, shifts electron transport

*Abbreviations:* Amplex Red, 10-acetyl-3,7-dihydroxyphenoxazine; BMPO, 5-*tert*-butoxycarbonyl-5-methyl-1-pyrroline *N*-oxide; $CaCl_2$, calcium chloride; $HbO_2$, oxyhemoglobin; $H_4B$, (6R)-5,6,7,8-tetrahydro-L-biopterin; HRP, horseradish peroxidase; $H_2O_2$, hydrogen peroxide; NOS1, neuronal nitric oxide synthase; $^{\bullet}NO$, nitric oxide; $O_2^{\bullet-}$, superoxide; SOD, superoxide dismutase; SPER-NO, (Z)-1-{*N*-(3-aminopropyl)-*N*-[4-(3-amino propylammonio)- butyl]amino}diazen-1-ium-1,2-diolate

* Corresponding author. Tel.: +1 410 706 0514; fax: +1 410 706 8184.
*E-mail address:* grosen@umaryland.edu (G.M. Rosen).

0006-2952/$ – see front matter © 2005 Elsevier Inc. All rights reserved.
doi:10.1016/j.bcp.2004.12.009

away from $O_2$, increasing $^{\bullet}NO$ production at the expense of $O_2^{\bullet-}$ [11]. Since $^{\bullet}NO$, $O_2^{\bullet-}$, and $H_2O_2$ initiate different cell signaling pathways [24,25], it is important to determine what impact L-arginine might have on NOS1 production of $O_2^{\bullet-}$ and $H_2O_2$. This paper describes a series of experiments designed to investigate the role of L-arginine in $H_4B$-bound NOS1 formation of $O_2^{\bullet-}$ and $H_2O_2$.

## 2. Materials and methods

### 2.1. Materials

NADPH, calmodulin, L-arginine, $N^{\omega}$-hydroxyl-L-arginine, calcium chloride ($CaCl_2$), $H_2O_2$, oxyhemoglobin ($HbO_2$), catalase, and horseradish peroxidase (HRP) were purchased from Sigma–Aldrich. Superoxide dismutase (SOD) was obtained from Roche Diagnostics. (Z)-1-{*N*-(3-aminopropyl)-*N*-[4-(3-amino propylammonio)-butyl]amino}diazen-1-ium-1,2-diolate (SPER-NO) was obtained from Midwest Research Institute. 10-Acetyl-3,7-dihydroxyphenoxazine (Amplex Red) was purchased from Molecular Probes. Amplex Red was dissolved in DMSO and stored under nitrogen at −80 °C until use. 5-*tert*-Butoxycarbonyl-5-methyl-1-pyrroline *N*-oxide (BMPO) was prepared as described in the literature [26,27]. All other chemicals were used as purchased without further purification.

### 2.2. Purification of NOS1

NOS1 was expressed and purified essentially as described by Roman et al. [28], with the modification that the culture volume was 500 mL rather than 1000 mL. The effluent from the ADP sepharose column was reconstituted with $H_4B$ (250 μM) at 4 °C. After overnight incubation on ice, this preparation was applied to an S-200 gel filtration column (Pharmacia) to remove excess $H_4B$ and to further purify the enzyme. The dimer peak was collected and concentrated. The enzyme concentration was determined by its carbon monoxide (CO)-difference spectrum, as described in [28], using an extinction coefficient of 100 $mM^{-1}$ $cm^{-1}$ at $\Delta\varepsilon$ = 444–475 nm.

### 2.3. Rate of nitric oxide production from NOS1

The initial rate of $^{\bullet}NO$ production by purified NOS1 was estimated using the $HbO_2$ assay [29]. The reaction was initiated by the addition of NOS1 (34 nM) to a cuvette, containing HEPES buffer (50 mM, 0.5 mM EGTA, pH 7.4), $HbO_2$ (20 μM), $CaCl_2$ (2 mM), calmodulin (100 U/mL), NADPH (150 μM), SOD (30 U/mL), catalase (100 U/mL), and L-arginine (0-100 μM) to a final volume of 0.5 mL at 23 °C. A UV–vis spectrophotometer (Uvikon, Model 940, Research Instruments, San Diego, CA) was used to monitor the conversion of $HbO_2$ to methemoglobin during the course of the reaction. Specifically, the increase in absorbance at 401 nm was used to quantify the reaction using an extinction coefficient of 60 $mM^{-1}$ $cm^{-1}$ at $\Delta\varepsilon_{401}$.

### 2.4. Spin trapping superoxide from NOS1

Spin trapping of $O_2^{\bullet-}$ from purified NOS1 was conducted by mixing all components to a final volume of 0.25 mL [30]. The reaction mixture was then transferred to a flat quartz cell and placed into the cavity of an EPR spectrometer (model E-109; Varian Associates Inc., Palo Alto, CA). The EPR quartz cell was open to the air. EPR spectra were recorded at room temperature. Instrument settings were: microwave power, 20 mW; modulation frequency, 100 kHz; modulation amplitude, 0.5 G; sweep time, 12.5 G/min; response time, 0.5 s. The receiver gain was $5 \times 10^4$. In a typical experiment, NADPH (150 μM) was added to potassium phosphate buffer (chelexed, 50 mM, pH 7.4, 1 mM EGTA, 1 mM DTPA) at 23 °C that contained NOS1 (70 nM), $CaCl_2$ (2 mM)/calmodulin (100 U/mL), BMPO (50 mM), $HbO_2$ (5 μM), and L-arginine or $N^{\omega}$-hydroxyl-L-arginine (from 0 μM to 50 μM). EPR spectra were recorded continuously after the addition of NADPH to the reaction mixture. The initial rate of $O_2^{\bullet-}$ generated was calculated by measuring in mm, the peak height of the first low-field peak of the EPR spectrum of BMPO-OOH. Given that this EPR spectrum is a composite of at least two conformers with unequal populations [27], it is very difficult to accurately estimate the concentration of BMPO-OOH, based on either the EPR spectral peak height or area under the spectral curve, standardized against a stable nitroxide, e.g., 3-carboxy-2,2,5,5-tetramethyl-1-pyrrolinyloxyl, of known concentration. We have, therefore, chosen to express the rate of $O_2^{\bullet-}$ production as mm/min.

### 2.5. Rate of hydrogen peroxide formation

Estimation of $H_2O_2$ production was obtained by fluorometric analyses (fluorometer, Hitachi model F2500, High Technologies America Inc., San Jose, CA). A modified method utilizing dye Amplex Red was adopted [31–33].

For control experiments, a microdialysis pump (CMA102 Microdialysis, Stockholm, Sweden) was used to infuse a stock $H_2O_2$ solution (0.1 mM). The concentration of commercial 30% $H_2O_2$ solution was calculated from light absorbance at 240 nm employing an extinction coefficient of 0.0436 $mM^{-1}$ $cm^{-1}$. Hydrogen peroxide was continuously infused at a rate of 50 pmol/min. The reaction contained Amplex Red (1 μM), HRP (5 U/mL) in sodium phosphate buffer (50 mM, 1 mM EGTA, pH 7.4) in the absence and presence of SPER-NO, generating $^{\bullet}NO$ at a rate of 400 pmol/min. The reaction was monitored as an increase in fluorescence of the dye at 585 nm with the excitation set at 550 nm.

An additional control experiment was undertaken. To a cuvette containing Amplex Red (1 μM), HRP (5 U/mL) in

the presence of either SPER-NO, affording •NO at a rate of 400 pmol/min or L-arginine (50 μM) in sodium phosphate buffer (50 mM, 1 mM EGTA, pH 7.4), $H_2O_2$ (100 pmol) was added stepwise to a final concentration of 700 pmol. The reaction was monitored as an increase in fluorescence of the dye at 585 nm with the excitation set at 550 nm.

The rate of $H_2O_2$ production by NOS1 in the presence of L-arginine or $N^{\omega}$-hydroxyl-L-arginine was conducted as follows. The reaction mixture contained NADPH (160 μM), $CaCl_2$ (2 mM), calmodulin (100 U/mL), BMPO (100 mM), L-arginine or $N^{\omega}$-hydroxyl-L-arginine (0–50 μM), and SOD (0.04 U/mL) in sodium phosphate buffer (50 mM, 1 mM EGTA, pH 7.4) into which Amplex Red (1 μM) and HRP (5 U/mL) was added. SOD was added to each reaction to suppress initial fluorescence seen from the inclusion of NADPH. The reaction was initiated by the addition of NOS1 (5 nM) into the reaction mixture. The initial rate of $H_2O_2$ generation was recorded as an increase in fluorescence of the dye at 585 nm with the excitation set at 550 nm. The fluorescence was calibrated by generating a standard curve with known concentrations of $H_2O_2$. A stock solution of $H_2O_2$ was diluted to 50 μM with water and used for calibration.

### 2.6. Rate of NADPH oxidation

Monitoring the oxidation of NADPH was performed in a reaction using potassium phosphate buffer (50 mM, pH 7.4, 1 mM DTPA, 1 mM EGTA), $CaCl_2$ (2 mM), calmodulin (100 U/mL), L-arginine or $N^{\omega}$-hydroxyl-L-arginine (0-50 μM), and NOS1 (70 nM) at room temperature to a total volume of 0.5 mL. The reaction was initiated by the addition of NADPH (150 μM). Initial rate of NADPH oxidation was estimated spectrophotometrically at 340 nm with an extinction coefficient of 6.22 $mM^{-1}$ $cm^{-1}$.

### 2.7. Curve fitting

Mathematical modeling, as shown in Figs. 1, 4–6 was performed using WinNonlin Pro (Version 4.0.1, Pharsight Corporation, Mountain View, CA 94040).

## 3. Results

### 3.1. $V_{max}$ and $K_m$ determination of NOS1

In our initial series of experiments, purified NOS1 production of •NO as measured by the $HbO_2$ assay [29] was used to determine $V_{max}$ and $K_m$. Although these values have been determined previously [28], the values for this specific enzyme preparation were beneficial to experiments described herein. The $V_{max}$ for •NO production from L-arginine was calculated to be 370 nmol/(min mg protein) and the $V_{max}$ of •NO production from $N^{\omega}$-hydroxyl-L-arginine was determined to be 357 nmol/(min mg protein). The $K_m$ for L-arginine for the NOS1 preparation used in this study was found to be 2.8 μM, the same as that previously reported for this *E. coli* derived NOS [28]. The $K_m$ for $N^{\omega}$-hydroxyl-L-arginine was determined to be 4.0 μM, slightly lower than the wide range of $K_m$ values from different sources of NOS (e.g., 6.6 μM from inducible nitric oxide synthase induced in RAW macrophages [8] and 25 μM from human kidney cells expressing NOS1 [34]), but consistently higher than that of L-arginine.

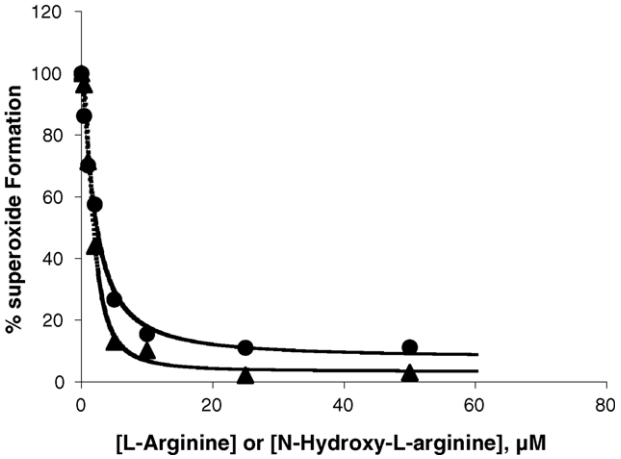


Fig. 1. The percent of the rate of $O_2^{\bullet-}$ generation by NOS 1 in the absence of $HbO_2$ as a function of L-arginine or $N^{\omega}$-hydroxyl-L-arginine concentration was fitted using an inhibitory sigmoidal function, $E = E_{max} - [(E_{max} - E_o)C\gamma]/(C\gamma + EC_{50}\gamma)$. $E$ is the % effect observed, $E_{max}$ the maximum effect, $E_o$ the baseline effect at saturated concentration of L-arginine or $N^{\omega}$-hydroxyl-L-arginine, and $EC_{50}$ is the concentration of L-arginine or $N^{\omega}$-hydroxyl-L-arginine required to inhibit 50% of the maximum observed effect. The filled circles are the observed data ($n = 3$) when L-arginine was used as the substrate and the line is from these fitted data, and $\gamma = 1.301$ is the shape parameter. The filled triangles are the observed data ($n = 3$) when $N^{\omega}$-hydroxyl-L-arginine was used as the substrate and the line is from these fitted data, and $\gamma = 3.6$ is the shape parameter.

### 3.2. Spin trapping superoxide from NOS1

We determined the initial rate of NOS1 generated $O_2^{\bullet-}$ at different L-arginine or $N^{\omega}$-hydroxyl-L-arginine concentrations, ranging from 0 μM to 50 μM. Spin trapping/EPR spectroscopy was the analytical method used for identifying NOS generated $O_2^{\bullet-}$ [35]. The choice of spin trap, BMPO, was based on the estimated second-order rate constant of 77 $M^{-1}$ $s^{-1}$ for reaction of $O_2^{\bullet-}$ with BMPO and the calculated half-life of the corresponding nitroxide, BMPO-OOH of 23 min, which exceeded those constants measured for 5,5-dimethyl-1-pyrroline *N*-oxide under the same experimental conditions [27]. As the concentration of L-arginine and $N^{\omega}$-hydroxyl-L-arginine increased from 0 μM to 50 μM, the rate of spin trapping $O_2^{\bullet-}$ decreased from $94 \pm 5$ mm/min to $11 \pm 1$ mm/min and from $84 \pm 13$ mm/min to $2.5 \pm 0$ mm/min, respectively. Percent control values were then calculated from these peak height/min values obtained at the various concentrations of substrate using 0 μM substrate as 100%. The percent rate

of spin trapping $O_2^{\bullet-}$, as a function of L-arginine or $N^{\omega}$-hydroxyl-L-arginine concentration was best fitted using the inhibitory sigmoidal function as implemented in WinNonlin, as shown in Fig. 1:

$$E = E_{max} - \frac{(E_{max} - E_o)C\gamma}{C^{\gamma} + EC_{50}\gamma}$$

where $E$ is the % rate of spin trapping $O_2^{\bullet-}$ observed, $E_{max}$ the maximum % rate of spin trapping $O_2^{\bullet-}$, $E_o$ the % rate of spin trapping $O_2^{\bullet-}$ at saturated concentration of L-arginine or $N^{\omega}$-hydroxyl-L-arginine, $C$ the concentration of L-arginine or $N^{\omega}$-hydroxyl-L-arginine, and $EC_{50}$ is the concentration of L-arginine or $N^{\omega}$-hydroxyl-L-arginine required to inhibit 50% of the maximum % rate spin trapping $O_2^{\bullet-}$ relative to $E_o$. The estimates of the $EC_{50}$ and $E_o$ for L-arginine and $N^{\omega}$-hydroxyl-L-arginine were $1.99 \pm 0.24$ μM and 7.7%, and $1.63 \pm 0.09$ μM and 3.3%, respectively. The value $\gamma$ is the shape parameter (Fig. 1) and estimates of $\gamma$ were found to be 1.3 and 1.8, respectively.

Given that $O_2^{\bullet-}$ and $^{\bullet}NO$ react at diffusion controlled rates [36], we investigated whether the decrease in the rate of spin trapping $O_2^{\bullet-}$ in the presence of increasing concentrations of either L-arginine or $N^{\omega}$-hydroxyl-L-arginine was the result of diminished availability of $O_2^{\bullet-}$ to react with the spin trap, or the direct effect of each substrate on the electron flow through the enzyme. To ascertain which of these possible pathways was operable, spin trapping experiments were performed in the presence of $HbO_2$, a probe that reacts with $^{\bullet}NO$. First, however, we needed to optimize experimental conditions to determine the lowest concentration of $HbO_2$ needed to completely scavenge $^{\bullet}NO$ generated by NOS. At concentrations of $HbO_2$, ranging from 3 μM to 10 μM, the rate of $^{\bullet}NO$ generated by NOS1, as measured by the $HbO_2$ assay [29] was maximal (data not shown). In contrast, concentrations of $HbO_2$ below 3 μM proved insufficient at removing all the $^{\bullet}NO$ that could react with the $O_2^{\bullet-}$ produced by NOS. To guarantee that all $^{\bullet}NO$ was scavenged, 5 μM of $HbO_2$ was used during the time course of the following experiments.

As the concentration of L-arginine and $N^{\omega}$-hydroxyl-L-arginine increased from 0 μM to 50 μM, the rate of spin trapping $O_2^{\bullet-}$ in the presence of $HbO_2$ (5 μM) decreased from $74 \pm 9$ mm/min to $13 \pm 3$ mm/min and from $58 \pm 9$ mm/min to $7 \pm 1$ mm/min, respectively. Data were best fitted using the same inhibitory sigmoidal function. Estimates of $\gamma$ for L-arginine and $N^{\omega}$-hydroxyl-L-arginine were 1.3 and 3.7, respectively. The calculated $EC_{50}$ and $E_o$ for both substrates were found to be similar (Table 1).

### 3.3. Rate of hydrogen peroxide formation

Before the rate of $H_2O_2$ formation by NOS1 could be estimated, a series of experiments were conducted to determine whether $^{\bullet}NO$ produced by the NOS1 metabolism of L-arginine or $N^{\omega}$-hydroxyl-L-arginine, or these substrates, per se, would interfere with the measurement of $H_2O_2$ using the HRP/Amplex Red fluorometric assay [31–33] as adapted from our earlier studies [15]. In the first set of control experiments, a microdialysis pump was used to infuse $H_2O_2$ (from a stock of 0.1 mM) into a cuvette (1 mL) containing HRP and Amplex Red. The rate of infusion was 0.5 μL/min, resulting in an $H_2O_2$ flux of 50 pmol/min. The reaction of $H_2O_2$ with HRP and consequently with Amplex Red was monitored fluorometrically as described in Section 2. This experiment was repeated in the presence of the $^{\bullet}NO$ donor SPER-NO, in which the rate of $^{\bullet}NO$ production was adjusted to 400 pmol/min. In the presence of $^{\bullet}NO$, the rate of fluorescence, in response to a constant influx of $H_2O_2$, was unchanged, as compared to those experiments in the absence of $^{\bullet}NO$, for the initial 2 min of the reaction (Fig. 2). Thereafter, there was a slight inhibition, which only became significant after 4 min. Since we are measuring initial rates, i.e., the scan time is only 1.5 min, of $H_2O_2$ production under our experimental conditions of a low $^{\bullet}NO$ flux, those typically found from NOS1 oxidation of L-arginine, accurate measurement of $H_2O_2$ generation from NOS1 should be obtainable.

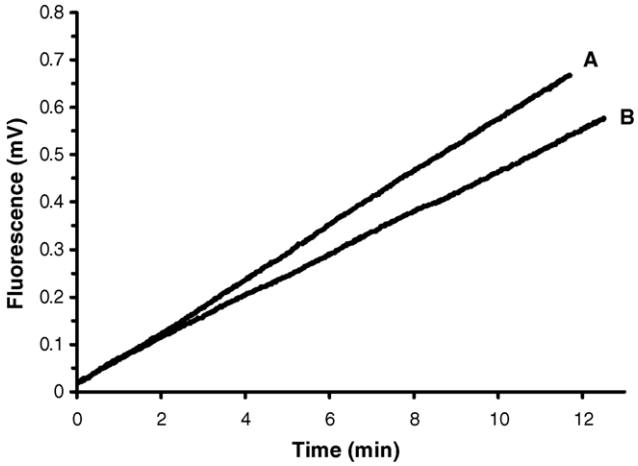


Fig. 2. Effect of $^{\bullet}NO$ on fluorometric determination of $H_2O_2$. (A) Infusion of $H_2O_2$ at a rate of 50 pmol/min. (B) Infusion of $H_2O_2$ at a rate of 50 pmol/min in the presence of a $^{\bullet}NO$ flux of 400 pmol/min. See Section 3 for more experimental detail.

In the second set of control experiments, a point-by-point calibration was performed in which 100 pmol of $H_2O_2$ was added stepwise to a final concentration of 700 pmol in the absence and presence of a $^{\bullet}NO$ flux of 400 pmol/min or L-arginine (50 μM). No significant change in the calibration curve was observed in the presence of $^{\bullet}NO$ or L-arginine as compared to control (Fig. 3). Supported by the results from these two sets of control experiments, we were confident that the low flux of $^{\bullet}NO$ from NOS1, at 5 nM, would not interfere with enzymatic production of $H_2O_2$, as assayed by this fluorometric method.

The initial rate of $H_2O_2$ generation by NOS1 in the presence of increasing L-arginine or $N^{\omega}$-hydroxyl-L-arginine (from 0 μM to 50 μM) was undertaken using the

Table 1
Summary of the $EC_{50}$ and $E_o$

| | L-Arginine | $N^{\omega}$-Hydroxyl-L-arginine | L-Arginine with $HbO_2$ | $N^{\omega}$-Hydroxyl-L-arginine with $HbO_2$ |
|---|---|---|---|---|
| NADPH consumption | | | | |
| $EC_{50}$ (μM)[a] | 7.5 ± 1.8 | 5.3 ± 1.9 | N.A.[c] | N.A.[c] |
| $E_o$ (%)[b] | 35.4 ± 4.6 | 30.3 ± 6.3 | N.A.[c] | N.A.[c] |
| Initial rate of $O_2^{\bullet-}$ production | | | | |
| $EC_{50}$ (μM)[a] | 2.0 ± 0.2 | 1.6 ± 0.1 | 1.3 ± 0.3 | 2.3 ± 0.2 |
| $E_o$ (%)[b] | 7.7 ± 3.1 | 3.3 ± 1.7 | 17.5 ± 4.5 | 16.0 ± 3.7 |
| Initial rate of $H_2O_2$ production | | | | |
| $EC_{50}$ (μM)[a] | 11.5 ± 3.7 | 13.4 ± 4.2 | N.A.[c] | N.A.[c] |
| $E_o$ (%)[b] | 43.7 ± 4.8 | 42 ± 6.6 | N.A.[c] | N.A.[c] |

[a] Values are expressed as ± of standard deviation derived from the fitting.
[b] The values of $E_o$ are expressed as % of the values without substrates.
[c] N.A. is none applicable.

fluorometric assay described in Section 2. As L-arginine and $N^{\omega}$-hydroxyl-L-arginine concentration increased from 0 μM to 50 μM, initial rates of $H_2O_2$ formation decreased from 203 ± 35 nmol/(min mg protein) to 111 ± 16 nmol/(min mg protein) for L-arginine and 203 ± 35 nmol/(min mg protein) to 134 ± 21 nmol/(min mg protein) for $N^{\omega}$-hydroxyl-L-arginine, respectively. The $V_{max}$ for $^{\bullet}NO$ production from L-arginine was calculated to be 370 nmol/(min mg protein) indicating that $H_2O_2$ generation in the absence of L-arginine can reach 55% of $^{\bullet}NO$ produced at saturation levels of L-arginine. And even at saturation concentrations of L-arginine, NOS1 can still produce $H_2O_2$ at the level of 30% of $^{\bullet}NO$ generated. Similarly, the $V_{max}$ of $^{\bullet}NO$ production from $N^{\omega}$-hydroxyl-L-arginine was determined to be 357 nmol/(min mg protein), indicating that $H_2O_2$ production in the absence of $N^{\omega}$-hydroxyl-L-arginine can reach 57% of $^{\bullet}NO$ generated at saturation concentrations of $N^{\omega}$-hydroxyl-L-arginine, and even at saturation levels of $N^{\omega}$-hydroxyl-L-arginine, NOS1 can still produce $H_2O_2$ at 38% of $^{\bullet}NO$ produced. To gain further insight into the electron flow by NOS1, these data were fitted as the percent of the initial rate of $H_2O_2$ production as a function of L-arginine or $N^{\omega}$-hydroxyl-L-arginine concentration using an inhibitory sigmoidal function:

$$E = E_{max} - \frac{(E_{max} - E_o)C}{C + EC_{50}}$$

The estimates of $EC_{50}$ and $E_o$ were 11.5 μM and 44% for L-arginine and 13.4 μM and 42% for $N^{\omega}$-hydroxyl-L-arginine (Figs. 4 and 5 and Table 1).

Of note, an interesting trend in $H_2O_2$ formation was observed at low concentrations of substrate (0–2.5 μM) (inserts in Figs. 4 and 5). Although a plot of $H_2O_2$ formation versus concentration reveals the same trend as that seen with $O_2^{\bullet-}$ formation for both substrates, at concentrations of L-arginine less than 1 μM, there is a spike in the generation of $H_2O_2$ by the enzyme from that produced at 0 μM. In the case of $N^{\omega}$-hydroxyl-L-arginine, concentra-

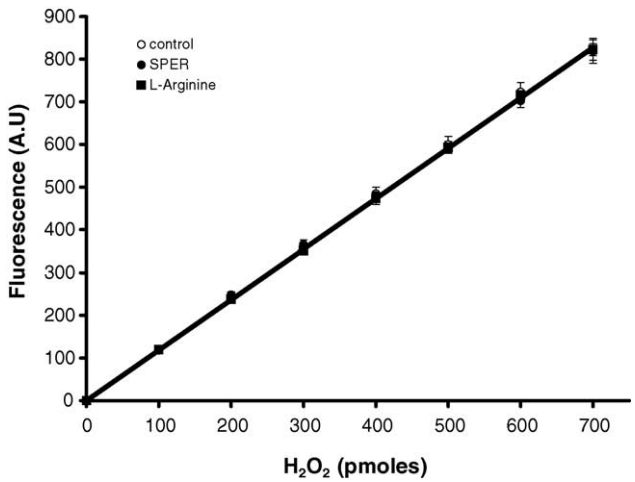


Fig. 3. A point-to-point calibration curve for the fluorometric measurement of $H_2O_2$ in the absence and presence of $^{\bullet}NO$ and L-arginine. Each point represents the mean ± S.D. of three independent experiments. See Section 3 for more experimental detail.

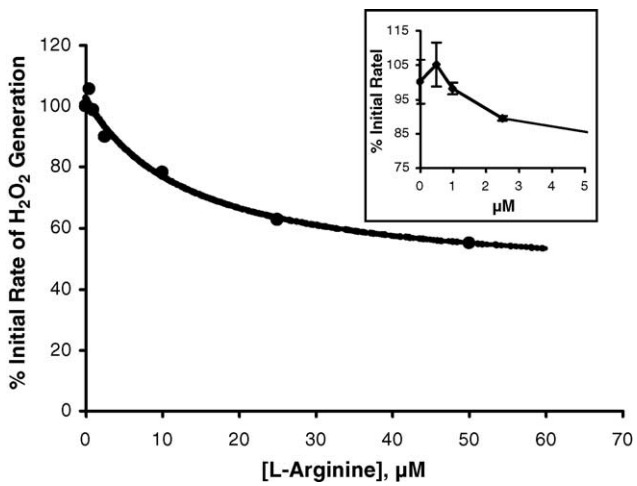


Fig. 4. The percent of the rate of $H_2O_2$ generation as a function of L-arginine concentration was fitted using an inhibitory function, $E = E_{max} - [(E_{max} - E_o)C]/(C + EC_{50})$. $E$ is the % effect observed, $E_{max}$ the maximum effect, $E_o$ the baseline effect at saturated concentration of L-arginine, and $EC_{50}$ is the concentration of L-arginine required to inhibit 50% of the maximum observed effect. The filled circles are the observed data ($n = 3$) and the line is from these fitted data. Insert: detailed view of the data points obtained between 0 μM and 2.5 μM of L-arginine.

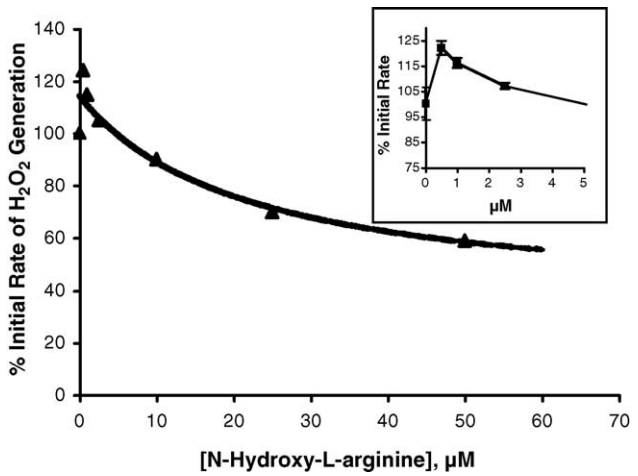


Fig. 5. The percent of the rate of $H_2O_2$ generation as a function of $N^{\omega}$-hydroxyl-*L*-arginine concentration was fitted using an inhibitory function, $E = E_{max} - [(E_{max} - E_o)C]/(C + EC_{50})$. $E$ is the % effect observed; $E_{max}$ the maximum effect; $E_o$ the baseline effect at saturated concentration of $N^{\omega}$-hydroxyl-L-arginine and $EC_{50}$ is the concentration of $N^{\omega}$-hydroxyl-L-arginine required to inhibit 50% of the maximum observed effect. The filled triangles are the observed data ($n = 3$) and the line is from these fitted data. Insert: detailed view of the data points obtained between 0 μM and 2.5 μM of $N^{\omega}$-hydroxyl-L-arginine.

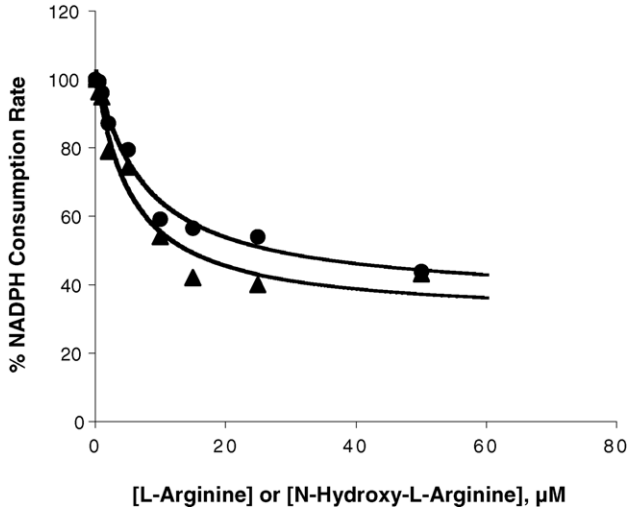


Fig. 6. The percent of NADPH consumption by NOS 1 as a function of L-arginine or $N^{\omega}$-hydroxyl-L-arginine concentration was fitted using an inhibitory function, $E = E_{max} - [(E_{max} - E_o)C]/(C + EC_{50})$. $E$ is the % effect observed, $E_{max}$ the maximum effect, $E_o$ the baseline effect at saturated concentration of L-arginine or $N^{\omega}$-hydroxyl-L-arginine, and $EC_{50}$ is the concentration of L-arginine or $N^{\omega}$-hydroxyl-L-arginine required to inhibit 50% of the maximum observed effect. The filled circles are the observed data ($n = 3$) when L-arginine was used as the substrate and the line is from these fitted data. The filled triangles are the observed data ($n = 3$) when $N^{\omega}$-hydroxyl-L-arginine was used as the substrate and the line is from these fitted data.

tions up to 2.5 μM generate significantly more $H_2O_2$ than that at 0 μM. We cannot fully explain this phenomenon at this time, but it warrants mention. These findings are currently being investigated further.

### 3.4. Rate of NADPH oxidation

Next, the effect, L-arginine or $N^{\omega}$-hydroxyl-L-arginine, had on the initial rate of NADPH oxidation was measured. As the concentration of L-arginine increased, stepwise from 0 μM to 50 μM, the rate of NADPH oxidation decreased from $1.88 \pm 0.32$ μmol/(min mg protein) to $0.82 \pm 0.03$ μmol/(min mg protein). Similarly, the rate of NADPH oxidation decreased from $1.69 \pm 0.06$ μmol/(min mg protein) in the absence of $N^{\omega}$-hydroxyl-L-arginine to $0.73 \pm 0.17$ μmol/(min mg protein) at 50 μM $N^{\omega}$-hydroxyl-L-arginine. These data are best fitted using an inhibitory sigmoidal function:

$$E = E_{max} - \frac{(E_{max} - E_o)C}{C + EC_{50}}$$

The parameters are the same as described above. The 100% effect represents the value of NADPH oxidation in the absence of substrate (Fig. 6). The estimates of the $EC_{50}$ and $E_o$ for L-arginine and $N^{\omega}$-hydroxyl-L-arginine were 7.5 μM and 35% and 5.3 μM and 30%, respectively.

## 4. Discussion

We have recently found that NOS1 generates $O_2^{\bullet -}$ and $H_2O_2$, the latter from the self-dismutation of $O_2^{\bullet -}$ as well as from the direct enzymatic reduction of $O_2$ [15]. As shown in Fig. 7, upon accepting an electron from $FMNH^{\bullet}$, $Fe^{2+}$ binds $O_2$, generating NOS–$(Fe^{3+})(O_2^{\bullet})$. In the absence of L-arginine or $N^{\omega}$-hydroxyl-L-arginine, this intermediate transfers an electron to $O_2$ releasing $O_2^{\bullet -}$ at a rate $v_1$. Alternatively, NOS–$(Fe^{3+})(O_2^{\bullet})$ can accept an electron, forming NOS–$(Fe^{3+})(O_2^{-})$, which then produces $H_2O_2$ with an overall rate $v_2$ (Fig. 7). We have found the rate of $O_2^{\bullet -}$ and $H_2O_2$ production – the ratio of $v_1$ and $v_2$ – to be regulated by $H_4B$ (15). However, in the presence of L-arginine, NOS1 production of $O_2^{\bullet -}$ decreases in a dose-dependent manner [11,12]. Yet, the impact L-arginine has on the formation of $O_2^{\bullet -}$ and $H_2O_2$ – the relationship between $v_3$ and $v_1$ and $v_2$ – remains unresolved (Fig. 7). Experiments described herein were aimed at exploring this fundamental question.

Our results suggest that the transfer of electrons from NADPH to $O_2$ in the absence of substrate is faster than the transfer of electrons for the oxidation of L-arginine or $N^{\omega}$-hydroxyl-L-arginine. These results confirm our earlier observation [11]. The $EC_{50}$ and $E_o$ are essentially the same when either L-arginine or $N^{\omega}$-hydroxyl-L-arginine is used as the substrate (Table 1), indicating that L-arginine and $N^{\omega}$-hydroxyl-L-arginine similarly influences the rate of NADPH consumption for NOS1.

We then turned our attention to the formation of $O_2^{\bullet -}$ by NOS1 in the presence of L-arginine or $N^{\omega}$-hydroxyl-L-arginine (Table 1 and Fig. 1). Since $^{\bullet}NO$ and $O_2^{\bullet -}$ react at $19 \times 10^9\ M^{-1}\ s^{-1}$ forming peroxynitrite ($ONOO^{-}$)

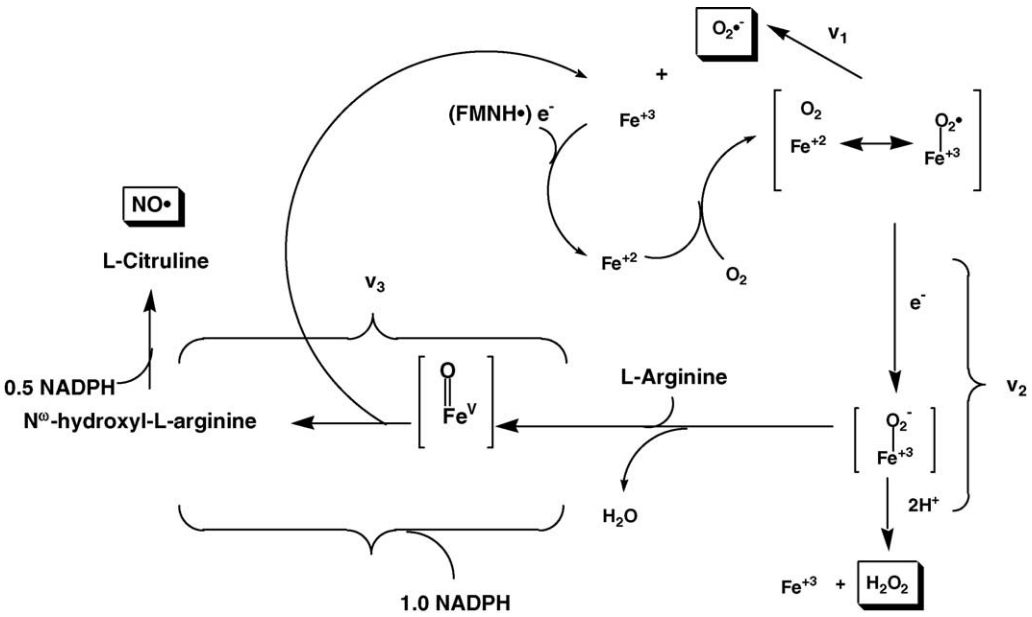


Fig. 7. A model depicting the formation of $O_2^{\bullet-}$ and $H_2O_2$ by NOS1 in the presence of L-arginine. We envision that $[Fe^{3+}–O_2^{\bullet}]$ releases $O_2^{\bullet-}$ with rate $v_1$. $[Fe^{3+}–O_2^{\bullet}]$ after accepting an additional electron forms $[Fe^{3+}–O_2^{-}]$, which can either release $H_2O_2$ with an overall rate of $v_2$ or rearrange to form the perferryl intermediate, $[Fe^{5+}{=}O]^{3+}$ that subsequently catalyzes the formation of $^{\bullet}NO$ from L-arginine at the expense of $H_2O_2$.

[36], the decrease in the rate of spin trapping $O_2^{\bullet-}$ with increased concentration of either L-arginine or $N^{\omega}$-hydroxyl-L-arginine (Fig. 1), may be due to the elimination of $O_2^{\bullet-}$ by $^{\bullet}NO$, generated from the oxidation of L-arginine or $N^{\omega}$-hydroxyl-L-arginine by NOS, rather than the direct effect of each substrate on the electron flow through the enzyme. To test this possibility, similar experiments were conducted in the presence of $HbO_2$ (5 μM). In the absence of substrates, the rates of spin trapping $O_2^{\bullet-}$, in the presence of $HbO_2$ were slightly smaller than those in the absence of $HbO_2$, indicating that $HbO_2$ had some effects on the spin trapping of $O_2^{\bullet-}$. However, since data were expressed as percent of the rates of spin trapping $O_2^{\bullet-}$ in the absence of substrates, the effects of $HbO_2$ would have minimal impact in the determination of $E_o$ and $EC_{50}$.

The $EC_{50}$ of $O_2^{\bullet-}$ formation were similar for both substrates in the absence or presence of $HbO_2$ (5 μM), whereas the $E_o$ was greater in the presence of the $^{\bullet}NO$ scavenger (Table 1). In the absence of $HbO_2$, the rate of spin trapping $O_2^{\bullet-}$ was underestimated at substrate concentrations higher than 5 μM due to the reaction of $^{\bullet}NO$ with $O_2^{\bullet-}$. Since the values of $EC_{50}$ were close to the values of $K_m$, these data indicated that the binding of L-arginine or $N^{\omega}$-hydroxyl-L-arginine diverts the flow of electrons toward the formation of $^{\bullet}NO$ and L-citrulline. However, even at saturated concentrations, L-arginine and $N^{\omega}$-hydroxyl-L-arginine did not completely inhibit the generation of $O_2^{\bullet-}$ as evidenced by the $E_o$ of 17% in the presence of $HbO_2$.

In a previous study, we reported on the use of the fluorometric assay, consisting of HRP and Amplex Red to measure the rate of $H_2O_2$ generation from NOS1 in the absence of L-arginine [15]. In the initial step, HRP is oxidized by $H_2O_2$ to afford Compound I. Amplex Red is further oxidized by Compound I. This reaction yields Compound II and the Amplex Red free radical. This intermediate then reacts with Compound II to regenerate HRP and the fluorescent resorufin [31–33]. This method has been shown to be applicable to estimating rates of $H_2O_2$ production from NOS1 in the absence of L-arginine [15]. However, a recent paper demonstrated that Compounds I and II of HRP react with $^{\bullet}NO$ with rate constants that may compromise measurements of $H_2O_2$ from this enzyme when L-arginine is present [37]. Reactions described in this paper [37] required the addition of $^{\bullet}NO$ into mixtures containing HRP and $H_2O_2$ in which $^{\bullet}NO$ was introduced as a bolus at 5 μM. We felt that there may be experimental conditions that would allow estimation of the rate of $H_2O_2$ production from NOS1 in the presence of L-arginine. Therefore, control experiments, as described in Section 3, demonstrated that $^{\bullet}NO$ produced by NOS1 did not affect the determination of direct $H_2O_2$ formation (Figs. 2 and 3).

Based on the results for direct $H_2O_2$ formation by NOS1 in the absence and presence of L-arginine and $N^{\omega}$-hydroxyl-L-arginine, the $EC_{50}$ and $E_o$ are not significantly different for both substrates, indicating that L-arginine and $N^{\omega}$-hydroxyl-L-arginine similarly influence the rate of $H_2O_2$ formation by NOS1. The $EC_{50}$ for the formation of $H_2O_2$ is much higher than that for the formation of $O_2^{\bullet-}$ (Table 1) and that for the $K_m$ of L-arginine and $N^{\omega}$-hydroxyl-L-arginine for the generation of $^{\bullet}NO$. These results indicate that the binding of either substrates slows the rate of $O_2^{\bullet-}$ formation ($v_1$) and the rate of $H_2O_2$ formation ($v_2$) by shifting the electron flow from NOS–$(Fe^{2+})(O_2)$ toward the formation of NOS–$(Fe^{3+})(O_2^{-})$ and then ultimately

toward the formation of the perferryl NOS–($Fe^{V}$=O) ($v_3$)(Fig. 7). This allows NOS to oxidize L-arginine or $N^{\omega}$-hydroxyl-L-arginine to L-citrulline and $^{\bullet}$NO. These findings also show that even at saturating concentrations of L-arginine or $N^{\omega}$-hydroxyl-L-arginine, a significant amount of $H_2O_2$ is still produced. In fact, the estimated value of $E_o$ for both substrates is approximately 60% of the initial rate of $H_2O_2$ formation in the absence of substrates (Table 1). These data combined with those from $O_2^{\bullet-}$ demonstrate that the addition of L-arginine or $N^{\omega}$-hydroxyl-L-arginine channel electron flow toward the formation of the perferryl, NOS–($Fe^{V}$=O), by increasing the rate $v_3$ at the expense of $v_1$ (Fig. 7). However, the greater value of $EC_{50}$ for the formation of $H_2O_2$ than that of $K_m$ of L-arginine or $N^{\omega}$-hydroxyl-L-arginine suggests that part of the generation of $H_2O_2$ is unrelated to the formation of the perferryl complex, perhaps coming from the reductase domain. This is consistent with the greater value of $E_o$ for $H_2O_2$ (~40%) compared with that of $O_2^{\bullet-}$ (~16%).

Experiments presented herein were designed to examine what impact L-arginine and $N^{\omega}$-hydroxyl-L-arginine has on NOS1 production of $O_2^{\bullet-}$ and $H_2O_2$. Several important observations are readily apparent from our studies. First, our data demonstrate that both L-arginine and $N^{\omega}$-hydroxyl-L-arginine slow the rate of NADPH consumption by NOS1. This results in diminished rates of $O_2^{\bullet-}$ and $H_2O_2$ formation, $v_1$ and $v_2$. L-Arginine and $N^{\omega}$-hydroxyl-L-arginine have the same influence in inhibiting the relative generation of $O_2^{\bullet-}$ and $H_2O_2$ by NOS1. Concomitant with this, both L-arginine and $N^{\omega}$-hydroxyl-L-arginine shift electron transfer to form L-citrulline and $^{\bullet}$NO more efficiently, e.g., higher $v_3$ (Fig. 7). Therefore, more $^{\bullet}$NO is generated with higher concentration of L-arginine or $N^{\omega}$-hydroxyl-L-arginine. Second, even at saturating concentrations of L-arginine or $N^{\omega}$-hydroxyl-L-arginine (50 μM), NOS1 still produces $O_2^{\bullet-}$ and $H_2O_2$. Undoubtedly, SOD and glutathione/glutathione peroxidase must regulate intracellular levels of $O_2^{\bullet-}$ and $H_2O_2$, respectively. When L-arginine or $N^{\omega}$-hydroxyl-L-arginine is used as an inhibitor of $O_2^{\bullet-}$ and $H_2O_2$, the $EC_{50}$ for $H_2O_2$ is much higher than that for $O_2^{\bullet-}$ (Figs. 1, 4 and 5 and Table 1). This finding indicates that L-arginine and $N^{\omega}$-hydroxyl-L-arginine are more efficacious inhibitors of $O_2^{\bullet-}$ than of $H_2O_2$. This observation is consistent with the fact that L-arginine or $N^{\omega}$-hydroxyl-L-arginine drives the formation of NOS–($Fe^{3+}$)($O_2^{-}$) and NOS–($Fe^{V}$=O), as these intermediates are responsible for the formation of $H_2O_2$ and $^{\bullet}$NO, which makes the formation of $O_2^{\bullet-}$ unfavorable (Fig. 7). At saturating concentrations of L-arginine or $N^{\omega}$-hydroxyl-L-arginine, $E_o$ for both $H_2O_2$ and $O_2^{\bullet-}$ does not reach zero, indicating there is always $H_2O_2$ and $O_2^{\bullet-}$ formed in the reaction. Also, the $E_o$ for $H_2O_2$ is higher than that of $O_2^{\bullet-}$. This observation sustains the theory that L-arginine or $N^{\omega}$-hydroxyl-L-arginine drives the formation of NOS–($Fe^{3+}$)($O_2^{-}$), leading to the production of $H_2O_2$, which is competitive with $^{\bullet}$NO and L-citrulline production. These findings are supportive of the proposed mechanism (Fig. 7) that the formation of $NO^{\bullet}$ and L-citrulline requires the intermediate NOS–($Fe^{V}$=O). Since this perferryl species is derived from NOS–($Fe^{3+}$)($O_2^{\bullet}$) and NOS–($Fe^{3+}$)($O_2^{-}$), one would expect the formation of $O_2^{\bullet-}$ and $H_2O_2$.

While it is premature to speculate as to the pharmacological significance of our findings, we would like to offer two possible scenarios. First, it has been found in this study that NOS1 generates $O_2^{\bullet-}$ and $H_2O_2$ in addition to $^{\bullet}$NO, even at saturating levels of L-arginine. The generation of these reactive oxygen species may have a deleterious pharmacological effect during the normal function of NOS1, especially if SOD and peroxidases, which would otherwise control cellular levels of these oxidants are compromised. For instance, $O_2^{\bullet-}$ can react with $^{\bullet}$NO to form $ONOO^{-}$, a potent oxidant that can elicit tissue injury [38–39]. Second, we have recently demonstrated that NOS1, in transfected kidney 293 cells, can differentially regulate the ERK signal transduction pathway, whose activity was controlled by varying cellular levels of $^{\bullet}$NO and $O_2^{\bullet-}$ [40].

## Acknowledgments

This research was supported in parts by Grants from the National Institutes of Health, EB-2034 (GMR and JW), AG-20445 (PT) and GM-52419 (LJR) and the Robert A. Welch Foundation Grant AQ1192 (LJR).

## References

[1] Nathan C, Xie Q-W. Regulation of biosynthesis of nitric oxide. J Biol Chem 1996;269:13725–8.
[2] Masters BSS, McMillan K, Sheta EA, Nishimura JS, Roman LJ, Martasek P. Neuronal nitric oxide synthase, a modular enzyme formed by convergent evolution: structure studies of a cysteine thiolate-ligand heme protein that hydroxylates L-arginine to produce $NO^{\bullet}$ as a cellular signal. Federation Am Soc Exp Biol J 1996;10:552–8.
[3] Marletta MA. Nitric oxide synthase structure and mechanism. J Biol Chem 1993;268:12231–4.
[4] Roman LJ, Martásek P, Masters BSS. Intrinsic and extrinsic modulation of nitric oxide synthase activity. Chem Rev 2002;102:1179–89.
[5] Siddhanta U, Prest A, Fan B, Wolan D, Rousseau DL, Stuehr DJ. Domain swapping in inducible nitric-oxide synthase. Electron transfer occurs between flavin and heme groups located on adjacent subunits in the dimer. J Biol Chem 1998;273:18950–8.
[6] Panda K, Gosh S, Stuehr DJ. Calmodulin activates intersubunit electron transfer in the neuronal nitric-oxide synthase dimer. J Biol Chem 2001;276:23349–56.
[7] Sagami I, Daff S, Shimizu T. Intra-subunit and inter-subunit electron transfer in neuronal nitric-oxide synthase. Effect of calmodulin on heterodimer catalysis. J Biol Chem 2001;276:30036–42.
[8] Stuehr DJ, Kwon NS, Nathan CF, Griffith OW, Feldman PL, Wiseman J. $N^{\omega}$-Hydroxy-L-arginine is an intermediate in the biosynthesis of nitric oxide from L-arginine. J Biol Chem 1991;266:6263–95.
[9] Rosen GM, Tsai P, Pou S. Mechanism of free-radical generation by nitric oxide synthase. Chem Rev 2002;102:1191–200.
[10] Pou S, Pou WS, Bredt DS, Snyder SH, Rosen GM. Generation of superoxide by purified brain nitric oxide synthase. J Biol Chem 1992;267:24173–6.

[11] Pou S, Keaton L, Surichamorn W, Rosen GM. Mechanism of superoxide generation by neuronal nitric-oxide synthase. J Biol Chem 1999;274:9573–80.
[12] Vásquez-Vivar J, Hogg N, Martásek P, Karoui H, Pritchard Jr KA, Kalyanaraman B. Tetrahydrobiopterin-dependent inhibition of superoxide generation for neuronal nitric oxide synthase. J Biol Chem 1999;274:26736–42.
[13] Yoneyama H, Yamamoto A, Kosaka H. Neuronal nitric oxide synthase. Biochem J 2001;360:247–53.
[14] Heinzel B, John M, Klatt P, Böhme E, Mayer B. $Ca^{2+}$/calmodulin-dependent formation of hydrogen peroxide by brain nitric oxide synthase. Biochem J 1992;281:627–30.
[15] Rosen GM, Tsai P, Weaver J, Porasuphatana S, Roman LJ, Starkov AA, et al. Role of tetrahydrobiopterin in the regulation of neuronal nitric-oxide synthase-generated superoxide. J Biol Chem 2002;277: 40275–80.
[16] Presta A, Weber-Main AM, Stankovich MT, Stuehr DJ. Comparative effects of substrates and pterin cofactor on the heme midpoint potential in inducible and neuronal nitric oxide synthases. J Am Chem Soc 1998;120:9460–5.
[17] Adak S, Wang Q, Stuehr DJ. Arginine conversion to nitroxide by tetrahydrobiopterin-free neuronal nitric-oxide synthase. Implications for mechanism. J Biol Chem 2000;275:33554–61.
[18] Klatt P, Schmidt K, Lehner D, Glatter O, Bächinger HP, Mayer B. Structural analysis of porcine brain nitric oxide synthase reveals a role for tetrahydrobiopterin and L-arginine in the formation SDS-resistant dimmer. EMBO J 1995;14:3687–95.
[19] Presta A, Siddhanta U, Wu C, Sennequier N, Huang L, Abu-Soud HM, et al. Comparative functioning of dihydro- and tetrahydropterins in supporting electron transfer, catalysis, and subunit dimerization in inducible nitric oxide synthase. Biochemistry 1998;37:298–310.
[20] Reif A, Fröhlich LG, Kotsonis P, Frey A, Bömmel HM, Wink DA, et al. Tetrahydrobiopterin inhibits monomerization and is consumed during catalysis in neuronal NO synthase. J Biol Chem 1999;274: 24921–9.
[21] McMillian K, Masters BSS. Optical difference spectrophotometry as a probe of rat brain nitric oxide synthase heme-substrate interaction. Biochemistry 1993;32:9875–80.
[22] Klatt P, Schmid M, Leopold E, Schmidt K, Werner ER, Mayer B. The pteridine binding site of brain nitric oxide synthase: tetrahydrobiopterin binding kinetics, specificity, and allosteric interaction with the substrate domain. J Biol Chem 1994;269:13861–6.
[23] Nishida CR, Ortiz de Montellano PR. Electron transfer and catalytic activity of nitric oxide synthases: chimeric constructs of the neuronal, inducible and endothelial isoforms. J Biol Chem 1998;273: 5566–71.
[24] Wolin MS. Interactions of oxidants with vascular signal systems. Arterioscler Thromb Vasc Biol 2000;20:1430–42.
[25] Dröge W. Free radicals in the physiological control of cell function. Physiol Rev 2002;82:47–95.
[26] Stolze K, Udilova N, Rosenau T, Hofinger A, Nohl H. Synthesis and characterization of EMPO-derived 5,5-disubstituted 1-pyrroline *N*-oxides as spin traps forming exceptionally stable superoxide spin adducts. Biol Chem 2003;384:493–500.
[27] Tsai P, Ichikawa K, Mailer C, Pou S, Halpern HJ, Robinson BH, et al. Esters of 5-carboxy-5-methyl-1-pyrroline *N*-oxide: a family of spin traps for superoxide. J Org Chem 2003;68:7811–7.
[28] Roman LJ, Sheta EA, Martásek P, Gross SS, Liu Q, Masters BSS. High-level expression of functional rat neuronal nitric oxide synthase in *Escherichia coli*. Proc Natl Acad Sci USA 1995;92:8428–32.
[29] Murphy ME, Noack E. Nitric oxide assay using hemoglobin method. Methods Enzymol 1994;233:240–50.
[30] Tsai P, Porasuphatana S, Pou S, Rosen GM. Investigations into the spin trapping of nitric oxide and superoxide: models to explore free radical generation by nitric oxide synthase. J Chem Soc Perkin Trans 2000;2:983–8.
[31] Mohanty JG, Jaffe JS, Schulman ES, Raible DG. A highly sensitive fluorescent micro-assay of $H_2O_2$ release from activated human leukocytes using a dihydroxyphenoxazine derivative. J Immunol Methods 1997;202:133–41.
[32] Zhou M, Diwu Z, Panchuk-Voloshina N, Haugland RP. A stable nonfluorescent derivative of resorufin for the fluorometric determination of trace hydrogen peroxide: applications in detecting the activity of phagocyte NADPH oxidase and other oxidases. Anal Biochem 1997;253:162–8.
[33] Zhou M, Panchuk-Voloshina N. A one-step fluorometric method for the continuous measurement of monoamine oxidase activity. Anal Biochem 1997;253:169–74.
[34] Abu-Soud HM, Wang J, Rousseau DL, Stuehr DJ. Stopped-flow analysis of substrate binding to neuronal nitric oxide synthase. Biochemistry 1999;38:12446–51.
[35] Weaver J, Tsai P, Cao G-L, Roman LJ, Rosen GM. Modified ferricytochrome c cannot be used to estimate nitric oxide synthase generation of superoxide. Anal Biochem 2003;320:141–3.
[36] Kissner R, Nauser T, Bugnon P, Lye PG, Koppenol WH. Formation and properties of peroxynitrite as studied by laser flash photolysis, high pressure stopped-flow technique, and pulse radiolysis. Chem Res Toxicol 1997;10:1285–92.
[37] Gover RE, Koshkin V, Dunford HB, Mason RP. The reaction rates of NO with horseradish peroxidase compounds I and II. Nitric Oxide 1999;3:439–44.
[38] Virág L, Szabó E, Gergely P, Szabó C. Peroxynitrite-induced cytotoxicity: mechanism and opportunities for intervention. Toxicol Lett 2003;140-141:113–24.
[39] Radi R, Peluffo G, Alvarez MN, Navailiat M, Cayota A. Unraveling peroxynitrite formation in biological systems. Free Radic Bio Med 2001;30:463–88.
[40] Raines KW, Cao G-L, Porsuphatana S, Tsai P, Rosen GM, Shapiro P. Nitric oxide inhibition of ERK1/2 activity in cells expressing neuronal nitric-oxide synthase. J Biol Chem 2004;279:3933–40.